2011 International Symposium on Nonlinear Theory and its Applications
NOLTA2011, Kobe, Japan, September 4-7, 2011

# Comparison of Brain Functional Networks and Internet Topologies by Complex Network Measures

Kenji Leibnitz†, Tetsuya Shimokawa†, Hiroaki Umehara†, and Tsutomu Murata†

†Brain ICT Laboratory, National Institute of Information and Communications Technology
588-2 Iwaoka, Iwaoka-cho, Nishi-ku, Kobe, Hyogo 651-2492, Japan
Email: {leibnitz,shimokawa,ume,benmura}@nict.go.jp

**Abstract**—Network structures can be found in various kinds of biological and engineered systems as medium for communication among the respective types of network nodes. The field of complex networks has paved the way to a generalized theoretical formalization of network topologies and these techniques have also been applied to investigate the connectivity of functional brain networks. In this paper, we discuss the method for extracting brain functional networks from fMRI measurement data and how to obtain characteristic complex network measures. We also apply the same techniques to ISP network topologies and explain fundamental similarities and differences.

## 1. Introduction

Recently, the progress in the field of network science has stimulated the study of a wide variety of network structures found in biological and engineered networks. The seminal work by Albert and Barábasi [1] and its introduction of the concept of scale-free networks has paved the way to a greater understanding of universal structures that can be observed in the connectivity of WWW documents, Internet routers, but also gene regulatory networks and brain functional networks [2]. Additionally, defining essential measures on connectivity permits quantifying and comparing different network topologies among each other. Especially, with the current redesign efforts toward a Future Internet, it is expected that understanding the mechanisms of biological networks is helpful for designing robust and adaptive *New Generation Networks* (NWGN) [3].

A biological network that shows remarkable abilities is that of the human brain. However, current neuroimaging techniques are not as advanced yet to observe the interactions among individual neurons. Methods like MEG or EEG can capture time series data at a resolution of milliseconds, but only for a limited number of sample points and not the entire brain. On the other hand, *functional MRI* (fMRI) can only capture data at a time resolution of seconds, but obtains complete 3-dimensional brain scans at a spatial unit of voxels (cubes of about 3mm in side). The rather low spatial resolution of fMRI leads to regarding nodes in brain networks as neuron groups rather than individual neurons, but it helps in understanding how different regions in the brain are activated during a cognitive task.

In this paper, we present a complex network analysis of brain networks from fMRI data and use complex network measures to compare their topologies with that of Internet providers. In line with other work [4, 5] we investigate typical complex network measures such as node degree, characteristic path length, clustering coefficient, and modularity to describe the network community structure [6, 7].

The paper is organized as follows. In Section 2 we summarize some essential features of complex networks as well as provide a definition of the measures we are applying. Then, in Section 3 we briefly explain the experiment which is used to extract functional MRI time data to network topologies. This is followed in Section 4 by a brief evaluation and the comparison with data of an Internet provider architecture. Finally, Section 5 concludes this paper.

## 2. Complex Networks and Their Measures

Complex networks describe random networks in real worlds based on specific topological features, such as heavy-tailed degree distribution, high clustering coefficient, modularity and community structure, etc. Two types of networks have been well studied in the past. *Scale-free networks* are characterized by a power-law degree distribution of their nodes, i.e., the number of other nodes to which any node is connected is not limited to a single scale, but varies over several orders of magnitude. On the other hand, *small-world networks* refer to those networks where any node can be reached from any other in few hops ("six degrees of separation"). Small-world networks have small diameter and high clustering coefficient.

Now, we briefly review the measures of complex networks that are used for characterizing a network consisting of the set of nodes $N$. Let $n$ and $\ell$ be the number of nodes and links, respectively. The matrix $A$ is the $n \times n$ dimensional adjacency matrix, i.e., $a_{ij} = 1$ if a link exists between nodes $i, j \in N$ and 0 otherwise. We list here the metrics of interest from [5] to which the reader is referred for further details.

- *Degree* $k_i$ of node $i$ describes the number of neighbors to which $i$ is connected.

$$k_i = \sum_{j \in N} a_{ij} \tag{1}$$

- *Characteristic path length L* of the network is the average of shortest paths $L_i$ of node $i$ to all other nodes

$$L = \frac{1}{n}\sum_{i\in N} L_i = \frac{1}{n}\sum_{i\in N}\frac{\sum_{j\in N, j\neq i} d_{ij}}{n-1} \tag{2}$$

with the shortest distance $d_{ij}$ between nodes $i$ and $j$.

- *Clustering coefficient C* of the network expresses how nodes linked to any given node $i$ are also linked among each other

$$C = \frac{1}{n}\sum_{i\in N} C_i = \frac{1}{n}\sum_{i\in N}\frac{2\,t_i}{k_i\,(k_i-1)} \tag{3}$$

where $C_i$ is the clustering coefficient of node $i$ and $t_i$ is its number of triangles among neighboring nodes: $t_i = \frac{1}{2}\sum_{j,h\in N} a_{ij}\,a_{ih}\,a_{jh}$.

We are interested in the modularity structure of the brain functional network and therefore also investigate the following metrics beside the traditional ones given above. Let us define the set of disjoint modules $M$ and $k_i(m)$ is the number of links between node $i$ and all nodes in $m \in M$.

- *Modularity Q* of the network describes how well the network is divided into modules of subnetworks

$$Q = \frac{1}{\ell}\sum_{i,j\in N}\left(a_{ij} - \frac{k_i k_j}{\ell}\right)\delta_{m_i,m_j} \tag{4}$$

where for $m_i, m_j \in M$ we have $\delta_{m_i,m_j} = 1$, if $m_i = m_j$ and 0 otherwise.

- *Participation coefficient* of a node $i$ is defined over the relative node degree in each module.

$$y_i = 1 - \sum_{m\in M}\left(\frac{k_i(m)}{k_i}\right)^2 \tag{5}$$

- *Within-module degree (z-score)* of node $i$ is

$$z_i = \frac{k_i(m_i) - \bar{k}(m_i)}{\sigma^{k(m_i)}} \tag{6}$$

where $\bar{k}(m_i)$ and $\sigma^{k(m_i)}$ are the mean and standard deviation of the within-module $m_i$ degree distribution.

## 3. Extraction of Networks from fMRI Data

Basically, fMRI measures the change in blood flow in the brain related to neural activity. Thus, the output from fMRI is related to the experiment design. In this work, we consider a simple *retinotopic* experiment where the primary visual cortex (V1) of the subject is stimulated by a checkerboard sequence. Three checkerboard images are presented for stimulation of the center, middle, and peripheral regions of V1 for 15s each, before a rest without stimulation, see Fig. 1. This sequence is repeated 6 times over 3 sessions.

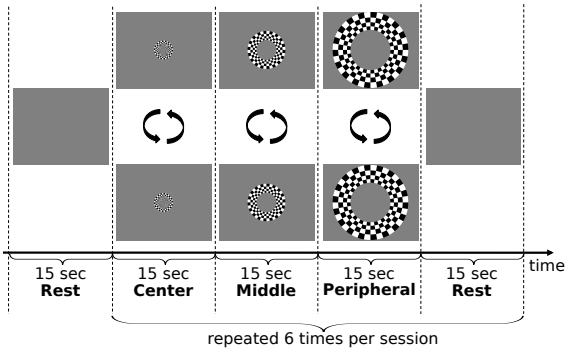


Figure 1: Epochs of retinotopy experiment

### 3.1. Types of Connectivity in Brain Networks

In [8], Sporns distinguishes between three different types of connectivity. We focus in this paper on functional connectivity, but briefly list all three types. *Anatomical connectivity* is the structural connectivity among neurons and remains rather static over short time scales, but may slowly change over time. Links are directional with respect to neural spike directions. *Functional connectivity* expresses the statistical dependence among spatially distributed neurons based on temporal correlation. Thus, functional links are undirected. Finally, *effective connectivity* describes the relationship between neural systems inferred by causal interaction models and considers directional links.

### 3.2. Processing Steps

The processing steps for extracting functional brain networks are sketched in Fig. 2. First, we extracted from fMRI measurements the time series for each voxel using the SPM Toolbox for MATLAB, which we also used to realign and normalize the data, but omitted smoothing. A *correlation matrix* is constructed among the time series of each pair of voxels $(x_1, x_2)$ and correlation is measured using Pearson's correlation coefficient as the fraction of the covariance of the two time series $V(x_1, t)$ and $V(x_2, t)$ over the product of their standard deviations, see Eqn. (7)

$$\rho_{x_1,x_2} = \frac{\langle V(x_1,t)\,V(x_2,t)\rangle - \langle V(x_1,t)\rangle\,\langle V(x_2,t)\rangle}{\sigma(V(x_1))\,\sigma(V(x_2))} \tag{7}$$

where $\sigma(V(x))^2 = \langle V(x,t)^2\rangle - \langle V(x,t)\rangle^2$.

Applying a masking threshold $r_c$ we obtain the *threshold matrix A* with entries $a_{i,j} = 1$ if the entry in the correlation matrix is above $r_c$ and 0 otherwise. This matrix can then be regarded as the adjacency matrix of the network graph of voxels which we use for obtaining our results.

## 4. Evaluation and Comparison with ISP Topologies

We also used the measurements available online from [9] of ISP topologies, in particular 3 large ISP networks:

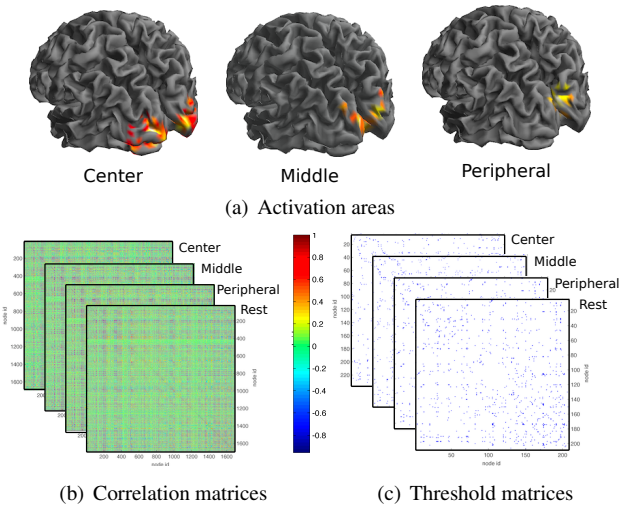


(a) Activation areas

(b) Correlation matrices (c) Threshold matrices

Figure 2: From fMRI scans to complex network measures

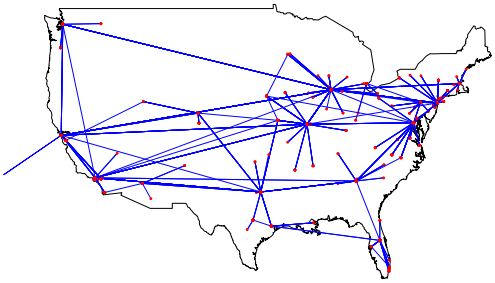

Figure 3: ISP topology of the AT&T network

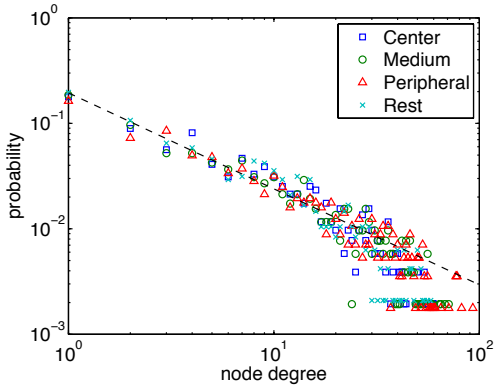


(a) Brain network with $r_c = 0.85$

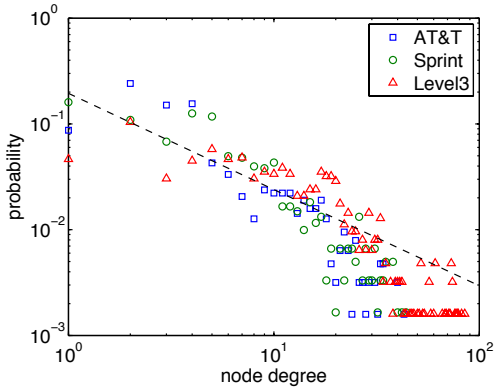


(b) ISP topologies

Figure 4: Node degree distribution

AT&T, Sprint, and Level 3. The adjacency lists were extracted to construct the adjacency matrices and we limit ourselves to only backbone and gateway routers. An example of the AT&T network topology is shown in Fig. 3.

### 4.1. Node Degree Distribution

The node degree distribution is shown in Fig. 4(a) for $r_c = 0.85$ for the brain network. In order to reduce the requirements on memory and processing time, we only selected each voxel at a step size of 5. As the figure shows, the shape of the distribution indicates a scale-free network regardless of the stimulation. Roughly the same shape can also be recognized from the degree distribution of ISP topologies in Fig. 4(b), where for the sake of comparison we added a linear fit from the brain data as dashed line.

### 4.2. Complex Network Measures

We performed analysis on further typical complex network measures shown in Table 1. The number of nodes $n$ and number of links $\ell$ lie in similar orders for both types of networks. Furthermore, the average node degree $\langle k \rangle$ is higher for brain networks and ascending from Rest to Center, Medium, Peripheral. Clustering coefficient $C$, characteristic path length $L$, and modularity $Q$ are also higher than ISPs and similar among all brain networks. Among the ISPs, the Level3 network has the highest $\langle k \rangle$ and $C$ while it has short path length and Sprint has the highest modularity.

### 4.3. Hierarchical Modularity

Hierarchical modularity [7] describes the community structure of the network and the roles that nodes play within it. Using participation coefficient and within-module degree, and partitioning the plot area as shown in Fig. 5, we can see that the brain networks all have similar structure, where the majority of nodes are located in categories R1, R2, R3 representing ultra-peripheral, peripheral, and non-

Table 1: Comparison of complex network measures

| **Network** | $n$ | $\ell$ | $\langle k \rangle$ | $C$ | $L$ | $Q$ |
|---|---|---|---|---|---|---|
| Rest | 478 | 2511 | 10.51 | 0.47 | 7.71 | 0.52 |
| Center | 515 | 2951 | 11.46 | 0.48 | 6.18 | 0.56 |
| Medium | 518 | 3345 | 12.92 | 0.50 | 7.52 | 0.53 |
| Periph. | 565 | 4164 | 14.74 | 0.51 | 6.25 | 0.53 |
| AT&T | 631 | 2078 | 6.59 | 0.10 | 5.04 | 0.27 |
| Sprint | 604 | 2274 | 7.53 | 0.15 | 4.18 | 0.48 |
| Level3 | 624 | 5300 | 16.99 | 0.26 | 3.35 | 0.33 |

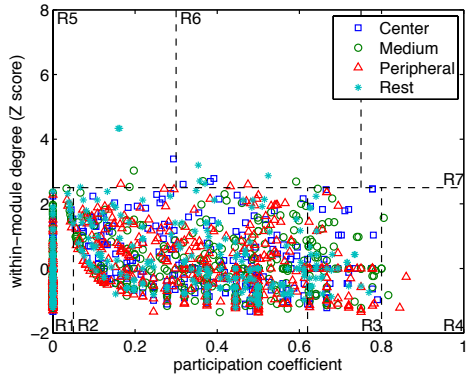


(a) Brain network with $r_c = 0.85$

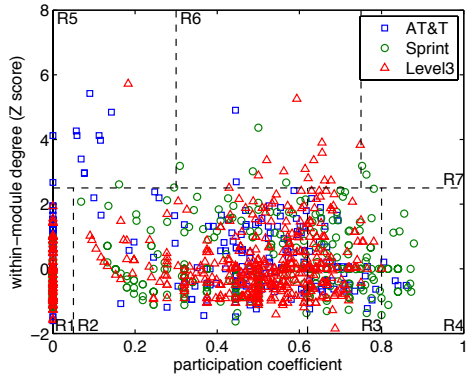


(b) ISP topologies

Figure 5: Hierarchical modularity

hub connector nodes, respectively. In comparison, the ISPs have mostly non-hub connectors. The Rest network has a few provincial (R5) and connector hubs (R6), but the AT&T network has more nodes in R5 and Level3 more in R6. Kinless hubs (R7) appear rarely and only for the Sprint network, which also has several non-hub kinless nodes (R4). Modularity is visualized for the Rest network graph using an optimized Fruchterman-Reingold layout in Fig. 6. The color and size of each node represent their module and category number R*i*, respectively.

## 5. Conclusion

In this paper we discussed the extraction of brain functional networks from fMRI data from a retinotopic experiment and compared their complex network measures with that of ISP topologies. We found that almost all brain networks had similar values, which can be attributed to the similarity of stimulations. Most metrics are comparable to ISP topologies, although with higher values. Analysis of the community structure revealed fewer hubs in brain networks than ISPs. In the future, we plan to study the structure and dynamics of brain functional networks during recognition tasks.

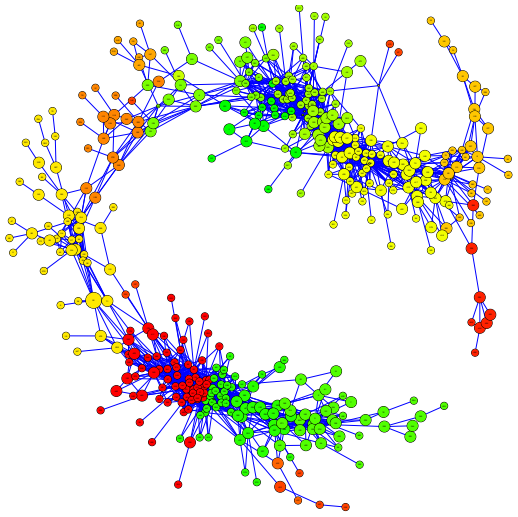

Figure 6: Visualization of modularity in Rest network


## Acknowledgments

The authors would like to thank Yusuke Morito for his help during the fMRI experiments and Shin'ichi Arakawa for his comments.


## References


[1] R. Albert and A.-L. Barabási, "Statistical mechanics of complex networks," *Rev. Mod. Phys.*, vol. 74, pp. 47–97, 2002.

[2] O. Sporns, *Networks of the brain,* MIT Press, 2010.

[3] H. Harai et al., "Design guidelines for new generation network architecture," *IEICE Trans. Commun.*, vol. E93-B, no. 3, pp. 462–465, 2010.

[4] V.M. Eguíluz et al., "Scale-free brain functional networks," *Phys. Rev. Lett.*, vol. 92, 018102, 2005.

[5] M. Rubinov and O. Sporns, "Complex network measures of brain connectivity: Uses and interpretations," *NeuroImage* vol. 52, pp. 1059-1069, 2010.

[6] R. Guimerá and L.A. Nunes Amaral, "Functional cartography of complex metabolic networks," *Nature*, vol. 433, pp. 895–900, 2005.

[7] D. Meunier et al., "Hierarchical modularity in human brain functional networks," *Front. Neuroinformatics*, vol. 3, no. 37, pp. 1–12, 2009.

[8] O. Sporns et al., "Organization, development and function of complex brain networks," *Trends Cogn. Sci.*, vol. 8, no. 9, pp. 418–425, 2004.

[9] "Rocketfuel: An ISP topology mapping engine", available online at: `http://www.cs.washington.edu/research/networking/rocketfuel/`.